

## The Evolutionarily Conserved Cassette Exon 7b Drives ERG's Oncogenic Properties

Samantha L. Jumbe<sup>\*,1</sup>, Sean R. Porazinski<sup>\*,1</sup>, Sebastian Oltean<sup>†</sup>, Jason P. Mansell<sup>\*</sup>, Bahareh Vahabi<sup>\*</sup>, Ian D. Wilson<sup>\*</sup> and Michael R. Ladomery<sup>\*</sup>

<sup>\*</sup>Faculty of Health and Applied Sciences, University of the West of England, Coldharbour Lane, Frenchay, Bristol BS16 1QY, United Kingdom; <sup>†</sup>Institute of Biomedical & Clinical Sciences, University of Exeter Medical School, St Luke's Campus, Heavitree Rd, Exeter, EX1 2LU, United Kingdom

### Abstract

The oncogene *ERG* encodes an ETS family transcription factor and is implicated in blood, vascular, and bone development and in prostate, blood, and bone cancer. The *ERG* gene is alternatively spliced; of particular interest is its cassette exon 7b which adds 24 amino acids, in frame, to the transcriptional activation domain. Higher exon 7b inclusion rates are associated with increased cell proliferation and advanced prostate cancer. The 24 amino acids encoded by exon 7b show evolutionary conservation from humans to echinoderms, highlighting their functional importance. Throughout evolution, these 24 amino acids are encoded by a distinct short exon. Splice-switching oligonucleotides based on morpholino chemistry were designed to induce skipping of *ERG* exon 7b in MG63 osteosarcoma and VCaP prostate cancer cells. Induction of exon 7b skipping reduced cell proliferation and invasion, increased apoptosis *in vitro*, and reduced xenograft growth *in vivo*. We also show that *ERG*'s exon 7b is required for the induction of tissue nonspecific alkaline phosphatase. Together, these findings show that the evolutionarily conserved cassette exon 7b is central to *ERG*'s oncogenic properties.

*Translational Oncology* (2019) 12, 134–142

### Introduction

The ETS-related gene (*ERG*), discovered in 1987, also known as the v-ets avian erythroblastosis virus E26 oncogene homolog, is a member of the highly conserved ETS family of transcription factors [1]. *ERG* is of fundamental importance in several developmental processes including hematopoiesis, chondrocyte maturation, and bone development and in apoptosis and cell migration [2]. The *ERG* gene is located on the q arm of chromosome 21 and expresses at least 30 splice variants [3,4]. Of particular interest are its cassette exons 7 and 7b; they are included in *ERG* transcripts at a higher rate in advanced prostate cancer [5,6]. Exon 7 encodes 27 amino acids and exon 7b encodes 24 amino acids, both in frame. These extra amino acids are added to the transcriptional activation domain (TAD) thought to influence the interaction of ERG with protein partners involved in transcriptional regulation [4]. Therefore, it is reasonable to assume that *ERG* splice isoforms that include or exclude the amino acids encoded by these cassette exons exhibit modified transcriptional activities and distinct biological functions.

Tissue nonspecific alkaline phosphatase (TNSALP) is key to securing an adequately mineralized bone matrix. Loss-of-function mutations in the *TNSALP* gene result in hypophosphatasia (HPP), and variants of the condition including perinatal HPP are lethal. A paucity of calcified

collagen is a striking feature of HPP, similar to rickets and osteomalacia [7]. The clear similarities in the phenotypic presentation of HPP, rickets, and osteomalacia suggest a role for vitamin D3 in the regulation of *TNSALP* expression. The active metabolite of vitamin D3, calcitriol (1,25D), promotes the development of mature bone-forming osteoblasts in which *TNSALP* expression is increased. How 1,25D serves to control *TNSALP* expression by osteoblasts is poorly understood, but it is becoming clear that 1,25D requires signaling cooperation from selected growth factors including TGF $\beta$  [8], EGF [9], and the pleiotropic lipid

Address all correspondence to: Michael R. Ladomery, Faculty of Health and Applied Sciences, University of the West of England, Coldharbour Lane, Frenchay, Bristol BS16 1QY, United Kingdom.

E-mail: [Michael.Ladomery@uwe.ac.uk](mailto:Michael.Ladomery@uwe.ac.uk)

<sup>1</sup> Joint first authorship.

Received 29 August 2018; Revised 7 September 2018; Accepted 7 September 2018

Crown Copyright © 2018 Published by Elsevier Inc. on behalf of Neoplasia Press, Inc. This is an open access article under the CC BY-NC-ND license (<http://creativecommons.org/licenses/by-nc-nd/4.0/>).

1936-5233

<https://doi.org/10.1016/j.tranon.2018.09.001>

mediator lysophosphatidic acid (LPA) and selected LPA analogues [10–12]. When the immature MG63 human osteoblast-like osteosarcoma cell line is co-stimulated with 1,25D and LPA, there is a demonstrable synergistic effect resulting in increased *TNSALP* expression. The fact that LPA and 1,25D can together enhance osteoblast maturation explains the effect of 1,25D on osteoblasts cultured in growth medium supplemented with serum, a rich source of LPA bound to the albumin fraction [13]. The potential role of ERG in *TNSALP* induction, and therefore in bone mineralization, of relevance to osteosarcoma and other cancers, has not yet been examined.

A critical role of *ERG* in bone and cartilage development and bone-related pathologies including bone cancer is rapidly emerging. A study carried out on chicken *ERG* reported that exon 7 is required for chondrocyte development. Skipping of this exon is prevalent in developing articular chondrocytes [14]. *ERG* lacking exon 7 maintains cells in an immature state and prevents maturation into hypertrophic cells and replacement of cartilage with bone, whereas expression of full-length *ERG* with exon 7 included promotes chondrocyte maturation. The role of the adjoining cassette exon 7b in chondrocyte development is not known. The *ERG* gene is also implicated in osteoarthritis. A murine model of osteoarthritis shows increased expression of *ERG* in articular cartilage, and treatment with a 1,25D analogue eldcalcitol increased its expression levels further [15]. Four weeks of histological assessment indicated a reduction in the progression of osteoarthritis correlated with increased *ERG* expression, suggesting that *ERG* contributes to resistance to osteoarthritis in the early stages of disease. The relevance of cassette exons 7 and 7b in the pathobiology of osteoarthritis is also not known.

In this study, splice-switching oligonucleotides (SSOs) were used to induce exon 7b skipping in the MG63 osteoblast-like cell line and for comparison also in the VCaP prostate cancer cell line. We show that ERG's exon 7b is involved in regulating cell proliferation and apoptosis and in invasion, consistent with its proposed oncogenic role [5,6]. Given the importance of bone formation in the progression of osteosarcoma (osteogenic sarcoma), we also set out to ascertain the potential involvement of the cassette exon 7b of the *ERG* oncogene in osteoblast maturation. *TNSALP* expression was induced in response to co-treatment with 1,25D and a phosphatase resistant analogue of LPA, (3S)1-fluoro-3-hydroxy-4-(oleoyloxy)butyl-1-phosphonate (FHBP), which we have previously shown enhances *TNSALP* expression [12,16]. We show that skipping of *ERG* exon 7b inhibits *TNSALP* induction, ascribing a new function to *ERG* and suggesting that *ERG* is also involved in bone mineralization control in a splice isoform-specific manner.

## Materials and Methods

All materials were obtained from Sigma-Aldrich unless otherwise stated.

### Cell Lines

MG63 (ECACC, human osteoblast-like osteosarcoma cells, catalogue no. 86051601) and VCaP cells (ECACC, human prostate cancer vertebral metastasis, catalogue no. 06020201) were grown in DMEM with 10% fetal bovine serum and 2 mM glutamine at 37°C

in 5% CO<sub>2</sub> in a humidified incubator. Where serum starvation was required, cells were cultured in phenol red-free DMEM:F12 supplemented with 100× stock of essential amino acids (5 mL per 500 ml medium) and glutamine (final concentration 2 mM).

### Vivo-Morpholinos

All vivo-morpholino SSOs were purchased from Gene Tools, LLC, USA. An SSO was designed against both the 5' and 3' splice sites of *ERG* exon 7b. The antisense sequence of the ERG exon 7b 5' splice site SSO (E7b5) was 5'-TCCGGTCCATGCTTTTGTGGGGACA-3', and for the ERG exon 7b 3' splice site (E7b3), it was 5'-AAGGAAAACA GACGTCCCCCACGUC-3'. The sequence for the control SSO, targeting an intron in the β-globin gene variant associated with β-thalassemia, was 5'-CCTCTTACCTCATTACAATTTATA-3'. Stocks of each vivo-morpholino were prepared in sterile PBS at a concentration of 0.5 mM. Each SSO has an octaguanidine dendrimer moiety to facilitate delivery for cellular uptake and was added directly to media. For experiments with VCaPs, the transfection reagent endoport (Gene Tools, LLC, USA) was used at 10 μM to facilitate uptake of SSOs.

### RNA Extraction and cDNA Synthesis

Total RNA was extracted using the total RNA isolation mini kit (Agilent Technologies Ltd.). All samples were treated with DNase on the columns using RNase-free DNase I provided in the kit. cDNA was synthesized from 0.2–1 μg of total RNA using 200 U MuLV reverse transcriptase (New England Biolabs), 40 U RNase inhibitor (human placenta) (New England Biolabs), 0.5 mM dNTP, 25 μM oligo-dT primers, and 10× reverse transcriptase buffer (500 mM Tris-HCl pH 8.3, 750 mM KCl, 30 mM MgCl<sub>2</sub>, 100 mM DTT) (New England Biolabs) in a final reaction volume 20 μl with added nuclease-free water as required (Qiagen).

### Semiquantitative Standard PCR and Gel Electrophoresis

Hot Start Taq 2× master mix (New England Biolabs) was used for standard PCR. Reactions were set up at room temperature in a final volume of 25 μl. The expression of *ERG* was measured using the primers listed in Table 1. The final concentration for each primer in the reaction was 0.4 μM. PCRs were run as follows: initial denaturation at 95°C for 30 seconds, then 30 cycles of 95°C for 30 seconds, 54°C for 1 minute, 68°C for 1 minute, and a final extension at 68°C for 5 minutes.

Gel electrophoresis was carried out using 1.5% agarose gels stained with 5 μl Midori Green Advance DNA stain (Geneflow) for every 100 ml of TAE. PCR products were loaded using purple 6× gel loading dye (New England Biolabs) and run at 150 V for the first 10 minutes then at 100 V until adequate migration was achieved. Gels were imaged on the Licor Odyssey Fc imaging system (Licor Limited). Splice isoform ratios were determined by measuring the relative brightness of PCR bands compared to each other using gel Image Studio Lite software (Licor Limited). Percent spliced in (PSI,  $\psi$ ) was determined as a ratio of the intensity of the top band (exon included) to the total signal of both bands.

**Table 1.** Primers Used for RT-PCR and RT-qPCR

	Forward Primer (5'-3')	Reverse Primer (5'-3')
ERG	GAATATGGCCTTCCAGACGTC AAC	GGTGGCCGTGACCGGTCCAGGCTG
Primers for RT-qPCR are listed below		
TNSALP	CGTCGATTGCATCTCTGGGC	GTCTCTTGCCTTGGTCTCG
U13397 (spike)	ACTCCGCTCAAGTGTTGAAG	GGTGGCTTGTAGCAATGAA

### Immunoblotting

Whole cell protein lysates were prepared from washed cell pellets using RIPA buffer [10 mM Tris-Cl (pH 8.0), 1 mM EDTA, 1% Triton X-100, 0.1% sodium deoxycholate, 0.1% SDS, and 140 mM NaCl] supplemented with protease inhibitor tablets (ThermoFisher). After a 30-minute incubation with periodical vortexing, lysates were centrifuged for 15 minutes at 12,000×g at 4°C for clarification. Samples were transferred to fresh tubes and quantified using the BCA kit (ThermoFisher) using a BSA standard curve.

Immunoblotting was carried out using 10 to 20 µg of total cell lysate. Samples were added to 2× Laemlli sample buffer and heated for 5 minutes at 100°C. Proteins were separated by handcast SDS-polyacrylamide gel electrophoresis gels on the Mini-PROTEAN Tetra vertical electrophoresis gel apparatus (Bio-Rad) and subsequently wet-transferred at 50 V for 2 hours on the Trans-Blot Turbo transfer apparatus (Bio-Rad). PVDF membranes were blocked with 5% (w/v) skimmed milk in Tris-buffered saline with 0.1% Tween-20 (TBST) for 1 hour at room temperature and probed with 1:1000 ERG (Abcam, mouse monoclonal, ab92513) and 1:10,000 β-actin primary antibodies (Abcam, polyclonal, ab8229) diluted in TBST overnight at 4°C. After three washes in TBST, membranes were incubated in 1:2000 HRP-linked anti-rabbit or anti-mouse IgG secondary antibody (New England Biolabs) for 2 hours at room temperature. Following a final three TBST washes, membranes were incubated in Luminata Forte Western HRP substrate (Millipore) for chemiluminescent detection for 2 minutes prior to image acquisition using the Licor Odyssey Fc imaging system.

### Real-Time Quantitative PCR (RT-qPCR)

RT-qPCR was performed in compliance with MIQE guidelines [17]. A SensiFAST SYBR Hi-ROX kit (BIOLINE UK, London) was used for qPCR. An exogenous spike made from the U13397 cDNA clone for the small RuBisCO subunit of *Arabidopsis thaliana* was produced using *in vitro* transcription (The *Arabidopsis* Information Resource, TAIR). Each RNA sample was spiked with 5 ng of the *RuBisCo* RNA spike prior to cDNA synthesis. During qPCR, the spike signal was measured in parallel to the genes of interest. Normalization was then carried out using the mass of the spike calculated from standard curve to calculate a multiplication factor for each sample relative to the sample with the highest spike expression. The mass of RNA for each gene of interest was then normalized using this multiplication factor. The primers were used at a final concentration of 200 nmol per reaction. The primer sequences are listed in Table 1. Serial dilutions of known amounts of the U13397 plasmid DNA were used to produce standard curves in order to facilitate quantitation. qPCR analysis was performed on a StepOne Plus real-time thermocycler (Life Technologies). Following a 2-minute activation step at 95°C, 45 cycles of 5 seconds at 95°C and 30 seconds at 57°C were carried out.

### Analysis of Cell Proliferation

After treatments, media were removed and cells were washed three times in PBS. The cells were then fixed in 3.7% (w/v) paraformaldehyde for 15 minutes at room temperature. The paraformaldehyde was discarded, and after three PBS washes, a solution of 0.1% (v/v) Triton X-100 was applied for 5 minutes to permeabilize the cells. Cells were then blocked in 3% FBS (in PBS) for 30 minutes before being incubated with Ki67 primary antibody (Abcam) in blocking solution (1:200) for 2 hours at room temperature. Three PBS washes were followed by incubation for 1 hour in fluorophore-conjugated secondary antibody (ThermoFisher Scientific, 1:2000) at room temperature, three more PBS washes, and a 2-minute incubation in 2 µg/ml Hoechst

3342. Images of each well were taken in six fields of view using the Eclipse 80i microscope (Nikon) using filters to detect the Ki-67 foci and Hoechst counterstain. ImageJ software was used to calculate the percentage of Ki67-positive cells.

### Apoptosis Assay

After seeding in 6-well plates, MG63 cells were treated with SSOs for 48 and 72 hours. Forty-five minutes prior to the end of the incubation period, the caspase 3/7 reagent (CellEvent) made up in prewarmed PBS was added. Images of six representative fields of view were taken for each sample using the 20× objective on the Eclipse 80i microscope (Nikon).

### Transwell Invasion Assay

For the invasion assay, PET inserts (membrane pore size, 8 µm; Millipore) were coated with 50 µl of Geltrex Matrix (ThermoFisher) diluted 1:1 in serum-free medium for at least 2 hours and up to 24 hours to create an artificial basement membrane. Inserts were set up in 24-well plates. MG63 cells were treated with SSOs for 24 hours and then harvested. Subsequently,  $1 \times 10^5$  cells in 100 µl serum-free medium were added to the upper chamber of the insert. A total of 600 µl of medium supplemented with 10% FBS was added to the lower chamber of the 24-well plate. Following 24 hours at 37 °C, the cells remaining on the upper membrane of the insert were removed and inserts washed in PBS. After 15-minute fixation in methanol and 2-minute staining with hematoxylin, the inserts were air dried prior to imaging of six representative fields of view using a camera attached to a light microscope (20× objective). The number of cells adhering to the lower membrane of the inserts was counted.

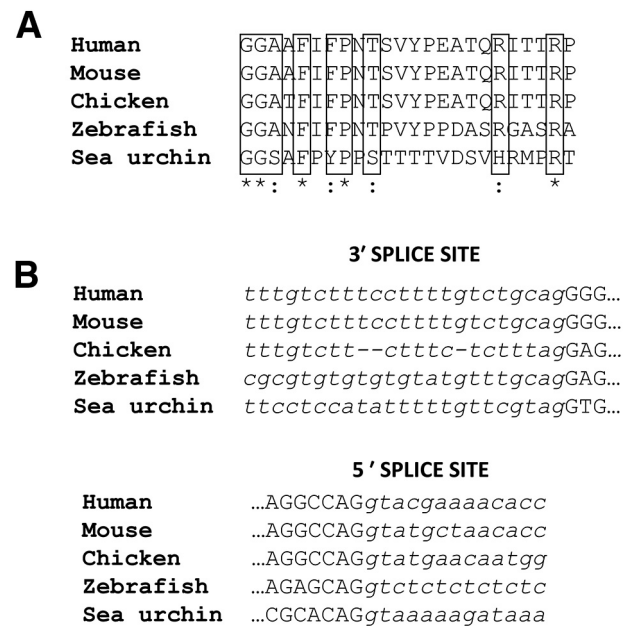


**Figure 1.** Evolutionary conservation of ERG's cassette exon 7b. (A) Alignment of the 24 amino acids encoded in frame by exon 7b in a range of species: *Homo sapiens* (human) NP\_001129626.1, *Mus musculus* (mouse) NP\_598420.1, *Gallus gallus* (chicken) XP\_015155736.1, *Danio rerio* (zebrafish) NP\_001008616.1, and *Strongylocentrotus purpuratus* (sea urchin) XP\_011672837.1. A putative ERK phosphorylation site is shown. (B) Alignment of a sample of corresponding genomic sequences surrounding the splice sites of the cassette exon. Sequences were obtained using BLAST (NCBI) and aligned with Clustal Omega.

**Mouse Xenograft Analysis**

Two-month-old male nude mice (CD1; Charles River, USA) were housed under pathogen-free conditions. All animal operations were approved by the Animal Ethics Committee, University of Exeter, U.K. A minimum of six mice were used per experimental group.

For heterotopic xenografts,  $7 \times 10^6$  MG63 cells resuspended in 100  $\mu$ l of PBS were injected subcutaneously into the right flank of mice. Tumors were measured with a caliper twice weekly, and tumor volume was calculated according to the formula:  $[(\text{length} + \text{width})/2] \times \text{length} \times \text{width}$ . Once tumors reached 3 mm by 3 mm in size, 12.5 mg/kg of SSO or PBS was administered by intraperitoneal injection twice weekly.

**Measurement of TNSALP Activity**

TNSALP activity can be measured by the generation of p-nitrophenol (p-NP) from p-nitrophenylphosphate (p-NPP) under alkaline conditions. Cells were seeded into 96-well plates in serum containing medium and given time to adhere to the cell culture vessel prior to being starved in serum-free phenol red-free DMEM/F12 medium overnight. Wells were dosed with 3  $\mu$ M of SSOs in the serum-free medium and incubated for 24 hours. Subsequently, FHBP and 1,25D were added to the relevant wells as well as an additional dose of SSO to maintain the expression of *ERG* exon 7b skipped isoforms. Following another 24-hour incubation, the treatment medium was removed and replaced with 100  $\mu$ l resazurin reagent made up in serum-

free medium (10  $\mu$ g/ml) 2-4 hours prior to the end of the incubation period in order to assess cell viability. The same volume was added to control wells containing no cells as a negative control. The plates were then read at 570 nm and 620 nm in a plate reader (FLUOstar OPTIMA, BMG Labtech) to obtain readings for cell viability.

The resazurin reagent was removed, and the monolayers were washed for 5 minutes in fresh serum-free medium to remove the residual resazurin and its metabolites. Following this, the medium was removed and the monolayers lysed with 50  $\mu$ l of TNSALP lysis buffer [25 mM sodium carbonate (pH 10.3) and 0.1% (v/v) Triton X-100]. After 2 minutes, each well was treated with 100  $\mu$ l of 15 mM p-NPP (di-Tris salt, Sigma-Aldrich) in 250 mM sodium carbonate (pH 10.3), 1 mM MgCl<sub>2</sub>. The cell culture plates were then returned to the cell culture incubator for 1 hour and transferred to the plate reader. An ascending series of p-NP concentrations (10-500  $\mu$ M) prepared in the incubation buffer were added to empty wells on the plate to enable quantification of product and the absorbance read at 405 nm. Reported total ALP activity was corrected to cell viability determined with the resazurin assay.

**Chromatin Immunoprecipitation Assay**

Chromatin immunoprecipitation was performed using the Imprint Chromatin Immunoprecipitation Kit (Sigma, UK) according to the manufacturer's protocol. Briefly,  $1 \times 10^6$  MG63 cells were incubated for 10 minutes with 1% formaldehyde at room temperature to allow

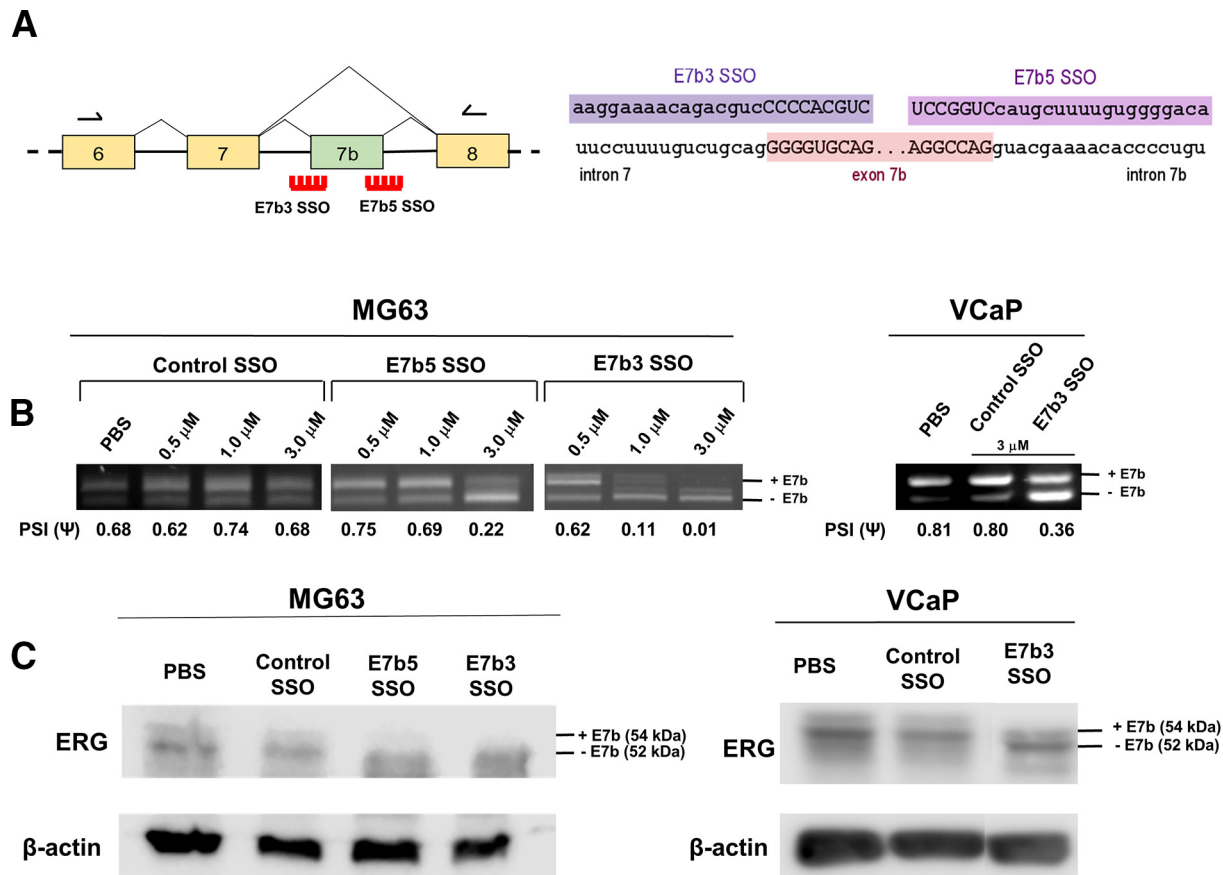


**Figure 2.** SSO-induced *ERG* exon 7b skipping in MG63 and VCaP cells. (A) The 5' and 3' splice sites of exon 7b were targeted using morpholino SSOs. The positions and sequences of the SSOs and the positions of *ERG* PCR primers are indicated. (B) Treatment with 3  $\mu$ M of the E7b3 SSO resulted in near-complete exon 7b skipping in MG63 and VCaP cells 24 hours after transfection. The percent spliced in (PSI,  $\psi$ ) ratio is shown. (C) Ninety-six hours after transfection with E7b5 and E7b3 SSOs, levels of ERG protein isoforms lacking the 24 amino acids (52 kDa) increased in both cell lines. A  $\beta$ -actin loading control was included in the western blot (cropped to highlight relevant bands).

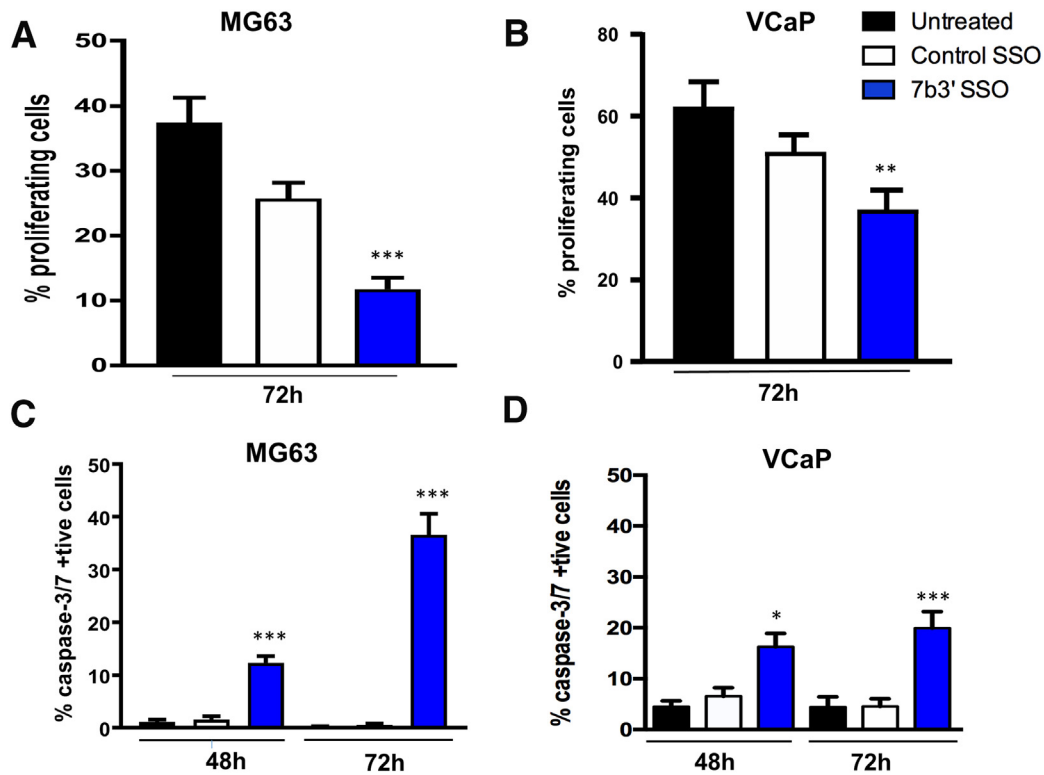


**Figure 3.** Effect of SSO-induced exon 7b skipping on cell proliferation (A,B) and apoptosis (C,D) in MG63 and VCaP cells. After 72 hours of treatment with  $3 \mu\text{M}$  SSO, Ki-67 expression was determined using immunofluorescent microscopy. Ki-67 foci were overlaid with DAPI. The graphs show the percentage of Ki-67-positive cells  $**P \leq .01$ ,  $N = 3$  repeats. Caspase 3/7-positive foci were quantified using immunofluorescent microscopy to determine apoptosis in MG63 (C) and VCaP (D) cells following treatment with  $3 \mu\text{M}$  SSO for 72 hours. The percentage of caspase 3/7-positive cells is shown ( $*P < 0.05$ ,  $**P < 0.01$ ,  $***P < 0.001$ ). Error bars show 95% confidence interval (95% CI);  $N = 3$  repeats.

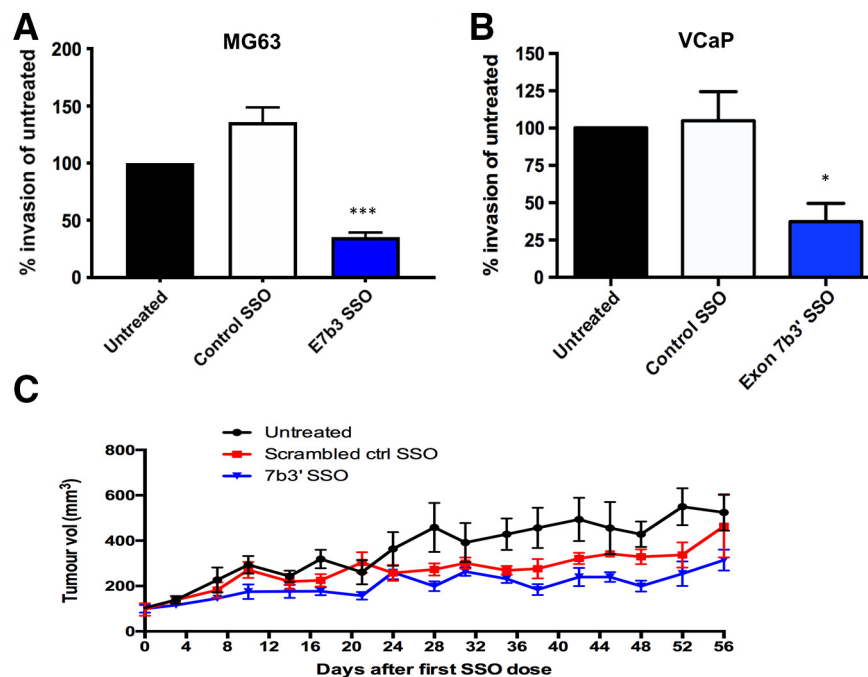


**Figure 4.** Effect of SSO-induced exon 7b skipping on invasion and xenograft growth. Transwell invasion assay in MG63 cells (A) and VCaP cells (B) 48 hours following SSO transfection. Fold change is relative to PBS control;  $N = 3$  repeats in each case. (C) A total of  $7 \times 10^6$  MG63 cells were injected subcutaneously into 2-month-old immunocompromised nude mice which were dosed intraperitoneally with saline, control SSO, or E7b3 SSO at 12.5 mg/kg twice weekly once tumors reached 3 mm by 3 mm in size. Tumors were measured with a caliper twice weekly over a period of 56 days. ( $*P < 0.05$ ,  $***P < 0.001$ ). Error bars in (A) and (B) show 95% confidence interval (95% CI);  $N = 3$  repeats. For the xenograft experiments (C) groups of six mice were used.

DNA to be cross-linked to protein. Cells were then lysed and DNA sheared to produce fragments of ~1000 bp using a sonicator, six pulses for 15 seconds at 50% power output followed by incubation on ice for 60 seconds after each pulse. The DNA-protein mixture was incubated in a well of a cell culture plate coated with 3 µg of anti-ERG antibody (Santa Cruz, UK), 1 µg RNA polymerase II antibody, or 3 µg nonspecific IgG at room temperature for 3 hours. This was followed by six washes with the IP wash buffer. The cross-linked DNA-ERG complexes were released using Proteinase K at 65°C for 15 minutes. The DNA was cleaned up and eluted using GeneElute Binding Column (Sigma, UK). PCR was then carried out using the following primers: ALPLF 5'-TCGCTGGAGGCATTCAAAC-3' and ALPLR 5'-CCCCTCTTAACAGGCAGAC-3'.

**Statistical Analysis**

The Kruskal-Wallis test and, where applicable, the Dunn's test were carried out. Significance levels are indicated by asterisks where \* =  $P < .05$ ,

\*\* =  $P < .01$ , and \*\*\* =  $P < .001$ . Data are reported as means, and error bars show 95% confidence intervals.

**Results**

**Evolutionary Conservation of ERG's Cassette Exon 7b**

We examined the evolutionary conservation of ERG's cassette exon 7b (Figure 1). We observed putative ERG orthologues across the evolutionary tree. We noted a 524-amino acid transcription factor in the sea urchin *Strongylocentrotus purpuratus* that aligns throughout the protein with human ERG (53% identity), with strongest conservation in the C-terminal ETS DNA-binding domain. We also observed strong conservation with sea urchin ERG in several pockets of the N-terminal regulatory domain, including the 24 amino acids encoded by exon 7b.

Next, we aligned the exon 7b 24 amino acids in ERG in several species including sea urchin and several vertebrates and noticed amino acid sequence conservation, especially in the first 10 amino acids. These

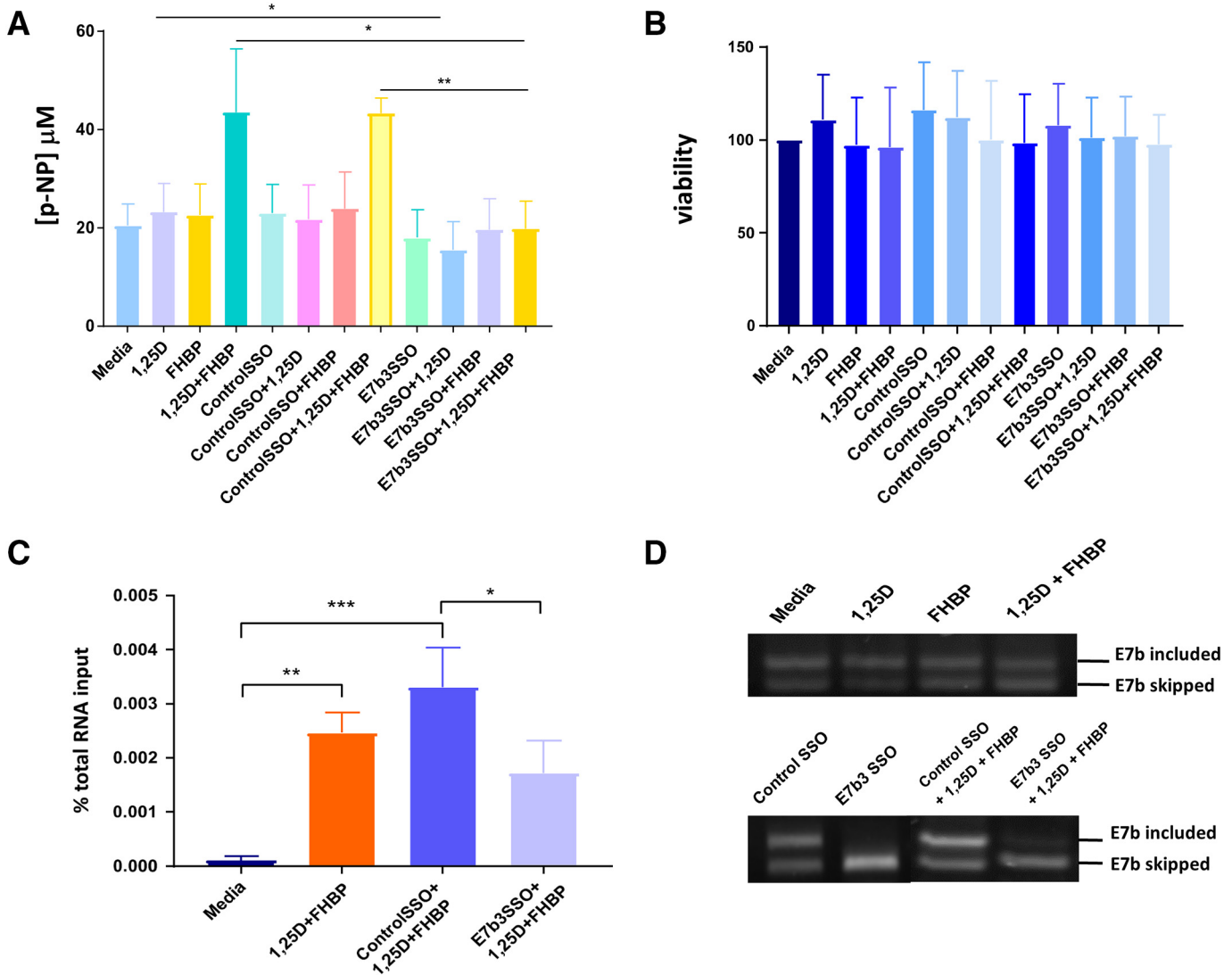


**Figure 5.** TNSALP induction is attenuated by SSO-induced skipping of exon 7b. (A) Treatment with 1,25D and FHBP induced TNSALP activity measured indirectly via the production of p-NP. (B) Cell viability measurements confirm that changes were not caused by reduced cell number or viability. (C) *TNSALP* expression levels were measured by qPCR, expressed as % of total RNA input. (D) The addition of 1,25D or FHBP alone did not induce exon 7b skipping.  $N = 5$  repeats in each case. (E) Analysis of the *TNSALP* promoter reveals the presence of at least one putative ERG binding site 960 bp upstream of the transcriptional start site. Primer positions and sequence are shown. (F) Chromatin immunoprecipitation analysis; *TNSALP* promoter DNA is present in the ERG immunoprecipitate. IgG, negative control; RNA polymerase II, positive IP control.

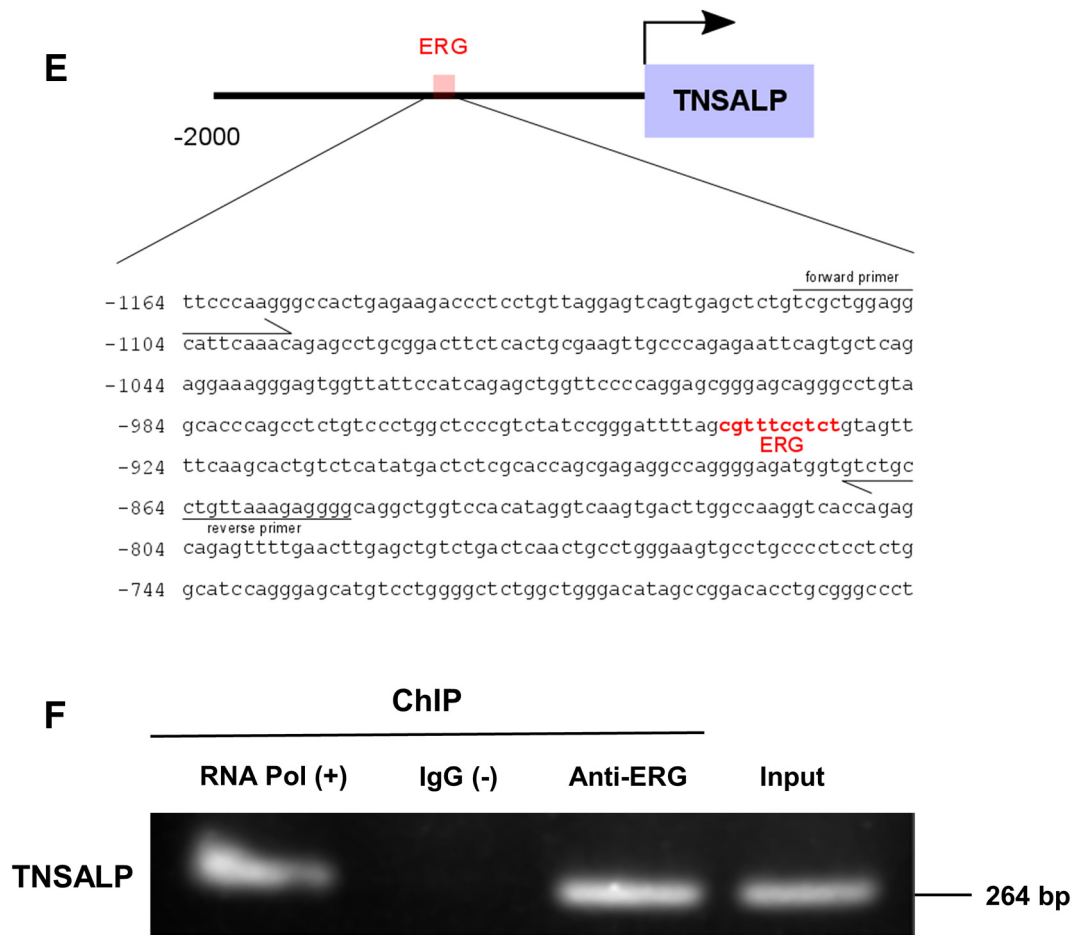


Figure 5. (continued).

include two aromatic residues, followed by a proline, and then a conserved threonine or serine. These amino acids are consistent with a potential ERK docking site, FxFP, known as 'DEF' (docking site for ERK FXF) [18]. At the end of the 24-amino acid sequence, there are also 2 conserved basic residues (Figure 1A).

We then examined whether or not these amino acids are encoded by a distinct exon throughout evolution. Analysis of genomic sequences in four species indicates that the 24 amino acids are, in all cases, encoded by a distinct 72-base exon. We suggest that the use of a small cassette exon to regulate the inclusion of these 24 amino acids is an ancient and common feature of the *ERG* gene (Figure 1B).

### SSOs Induce *ERG* Exon 7b Skipping

SSOs were designed to target, through sterical hindrance, the splice acceptor (E7b3) and donor (E7b5) sites of exon 7b in *ERG* (Figure 2A). MG63 osteosarcoma cells were treated with 0.5, 1, and 3  $\mu\text{M}$  of each SSO for 24 hours, after which the rates of *ERG* exon 7b inclusion were measured (Figure 2B). A control SSO was included in addition to a PBS vehicle control. The most efficient exon skipping was observed with the E7b3 SSO at 3  $\mu\text{M}$  with almost undetectable exon 7b [0.01 PSI ( $\psi$ ), where  $\psi$  is the proportion of exon inclusion], compared to 0.22  $\psi$  obtained with the E7b5 SSO. There was detectable exon skipping at the lower 1- $\mu\text{M}$  dose with the E7b3 SSO. The control SSO did not cause any significant changes to *ERG* exon 7b skipping. Next, we tested the most efficient SSO, E7b3, in VCaP prostate cancer cells and observed a similar, convincing shift in PSI value from 0.81 to 0.32 using 3  $\mu\text{M}$  E7b3. Exon 7b skipping was confirmed at the protein level (Figure 2C).

### *ERG* Exon 7b Skipping Reduces Cell Proliferation and Invasion, Increases Apoptosis, and Reduces Xenograft Growth

Having established that exon 7b skipping could be achieved with SSOs, we proceeded with the best performing SSO E7b3 and examined the biological roles of exon 7b in MG63 and VCaP cells using a range of cell biology assays. SSO-induced exon 7b skipping resulted in a significant decrease in cell proliferation in both cell lines measured via Ki-67 staining (Figure 3, A and B). In parallel, we observed a significant increase in apoptosis as a result of exon 7b skipping, measured through caspase 3/7 staining (Figure 3, C and D).

SSO-induced exon 7b skipping also resulted in reduced cell invasion assayed through a Transwell assay (Figure 4, A and B). We also performed a mouse xenograft experiment (Figure 4C). A total of  $7 \times 10^6$  MG63 cells were injected subcutaneously into 2-month old nude mice. Tumor volumes were measured over a period of 56 days. Whereas we did notice a partial effect with the control SSO, the E7b3 SSO achieved the greatest reduction in tumor growth. Taken together, these results are consistent with exon 7b inclusion driving the oncogenic properties of ERG.

### *TNSALP* Induction Is Attenuated by Exon 7b Skipping

Next, we considered the effect of exon 7b skipping on the ability of osteoblast-like MG63 cells to differentiate, measured through the expression of TNSALP. Serum-starved MG63 cells were first treated with SSOs for 24 hours. After 24 hours, the cells were treated with 1,25D and FHBP and given an additional dose of SSO. After a further 24 hours, alkaline phosphatase activity was assessed using the

well-established method of measuring *p*-nitrophenyl phosphate (*p*-NPP) conversion to *p*-nitrophenol (*p*-NP), producing a yellow color quantified by measuring absorbance at 405 nm. As expected, the co-stimulation of MG63 cells with 1,25D and FHBP resulted in an increase in *p*-NP production consistent with TNSALP induction. In the presence of E7b3 SSO, the increase of *p*-NP was significantly lower compared to the 1,25D and FHBP co-treatments alone. Control SSO with 1,25D and FHBP did not cause a significant attenuation of *p*-NP levels (Figure 5A). A resazurin cell viability assay confirmed that changes observed with the TNSALP activity assay were not due to changes in cell number or viability (Figure 5B).

RT-qPCR was used to measure the expression of the *TNSALP* gene. We observed significantly increased expression in the 1,25D and FHBP co-treated cells and in the presence of the control SSO. The reduction of *TNSALP* expression in the presence of E7b3 SSO was statistically significant (Figure 5C), in agreement with the TNSALP assay results. To confirm that *ERG* exon 7b skipping was occurring both prior to and after 1,25D and FHBP treatment, a standard PCR analysis of *ERG* exon 7b skipping was carried out. Exon 7b skipping was detected in E7b3 SSO-treated cells (Figure 5D). Treatment with 1,25D and FHBP, either alone or in combination, did not alter *ERG* exon 7b skipping rates.

We examined the *TNSALP* promoter for the presence of putative ERG binding sites (conforming to the core GGAA sequence, Figure 5E). We noted the presence of at least one putative ERG binding site, AGAGGAAACG, 930 bp upstream of the transcription start site. We designed primers flanking this site, covering 264 bp of promoter sequence, and performed a chromatin immunoprecipitation assay (Figure 5F). ERG co-immunoprecipitated with this sequence but not with the GAPDH promoter (data not shown), suggesting that ERG binds to the *TNSALP* promoter, directly regulating its transcription.

## Discussion

Alternative splicing of *ERG* cassette exon 7b has previously been shown to alter ERG's biological functions. Cell proliferation increases when exon 7b is included [5], and we have previously reported that higher exon 7b inclusion rates are associated with advanced prostate cancer [6]. We observe that the 24 amino acids encoded in frame by exon 7b in humans are conserved throughout evolution and are encoded by a distinct, short 72-base exon. In humans, inclusion of this cassette exon is likely regulated by trans-acting splice factors whose identity remains to be determined. ERG's contribution to the regulation of cell proliferation, apoptosis, and differentiation is, we suggest, regulated by alternative splicing. The physiological importance of exon 7b is further underlined by the presence of an evolutionarily conserved putative ERK (extracellular signal regulated, mitogen-activated protein kinase) docking site (FxFP) within the 24 amino acids encoded by exon 7b [19]. The phosphorylation of ERG is required to promote the migration of prostate cancer cells and the transcription of migration-associated genes [20]. ERG phosphorylation is stimulated via VEGF through the MAPK/ERK cell signaling pathway, promoting sprouting angiogenesis, a hallmark of cancer [21].

We designed SSOs based on morpholino chemistry that targeted both splice sites of exon 7b. The SSO that targets the 3' splice site was the most efficient. Having established an appropriate dose, we observed that, 48 hours after transfection, the 3' splice site SSO (E7b3) achieved near complete skipping of exon 7b. SSO-induced exon 7b skipping significantly reduced cell proliferation, increased apoptosis, and reduced cell invasion. We also performed a xenograft experiment using MG63 cells. We observed that the E7b3' SSO significantly reduced the growth

of the xenografted cells. SSOs that prevent the inclusion of exon 7b could therefore have therapeutic potential.

We also wanted to examine if cassette exon 7b contributes to the maturation of osteoblast-like MG63 osteosarcoma cells, measured via the activation of TNSALP. Addition of 1,25D and FHBP to the MG63 was used to establish a maturation model in which increased TNSALP activity was observed [12,16]. There was a significant attenuation of TNSALP induction in the presence of E7b3 SSO, confirmed by reduced mRNA levels and at a protein level via decreased *p*-NP production. A study by Iwamoto and colleagues had previously identified a reduction in alkaline phosphatase activity and mineralization when the C-1-1 ERG isoform lacking the 81-bp cassette exon 7 was expressed [14]. Our findings suggest that exon 7b is also required for the induction of alkaline phosphatase activity. Exons 7 and 7b both encode for part of the TAD domain of ERG that, we presume, modulates the transactivation activities of the ERG transcription factor during development. In both mouse and chicken models, *ERG* is involved in chondrocyte development in a splice isoform-specific manner [14,22,23]. However, the extent to which both exon 7 and 7b skipping is required, the effect of each cassette exon on ERG's transcriptional activity, and whether or not the regulation of their alternative splicing is coordinated are not yet known.

Previous characterization of the *TNSALP* promoter revealed the presence of binding sites for the transcription factor SP1 [24–26]. The inhibition of SP1 promoter binding by mithramycin A in the presence of 1,25D/FHBP co-treatment reduced the levels of *TNSALP* [27], suggesting that the SP1 promoter binding sites may have biological relevance. It is conceivable that ERG also activates *TNSALP* transcription directly, in an isoform-specific manner (ERG + exon 7b), and this is consistent with our chromatin immunoprecipitation result. Alternatively, ERG's involvement in *TNSALP* activation could also be indirect; there is evidence that ERG is involved in the activation of SP1 itself, and ERG physically interacts with SP1 [28]. The precise mechanisms remain to be determined, but we propose that ERG and SP1 transcription factors work together to regulate *TNSALP* expression and that *ERG* plays a role in the regulation of bone mineralization via interaction with 1,25D and LPA-sensitive pathways. The ability of ERG to activate *TNSALP* and therefore to promote bone matrix mineralization is of significance to the development and progression of osteosarcoma [29,30] and potentially of other cancers in which ERG is implicated.

In conclusion, this study affirms the evolutionary conservation of ERG's cassette exon 7b and of the 24 amino acids it encodes. We confirm the importance of exon 7b in regulating cell proliferation, apoptosis, migration, and invasion. We also present a novel role for the ERG transcription factor and its cassette exon 7b in the induction of *TNSALP*. We have successfully designed SSOs that target *ERG* exon 7b, causing efficient skipping of the exon. SSOs that cause skipping of ERG's cassette exon 7b could provide a novel therapeutic avenue.

## Author contributions

S. J. and S. R. P. conducted the experimental work. B. V., S. O., J. P. M., and I. D. W. contributed to supervision, and M. R. L. was the PI.

## Conflict of Interest

None of the authors have any potential conflicts of interest to disclose.

## Acknowledgements

The authors thank Dr. Lee Spraggon Memorial Sloan Kettering Cancer Center, USA, for advice in designing and testing the SSOs.



M. L. is a member of the European Organisation for Research and Treatment of Cancer, Pathobiology Group. S. L. J. was supported by a scholarship from the Malawi Government Scholarship Fund. S. P. was supported by a Research Innovation Award from Prostate Cancer UK, ref. RIA-030-15. We are also very grateful to GeneTools, LLC, and in particular to Jim Summerton for technical advice and the provision of reagents.

## References

- [1] Rao VN, Papas TW, and Reddy ES (1987). A human ets-related gene on chromosome 21: alternative splicing, polyadenylation, and translation. *Science* **237**, 635–639.
- [2] Adamo P and Ladomery MR (2015). The oncogene *ERG*: a key factor in prostate cancer. *Oncogene* **35**, 403–414.
- [3] Owczarek CM, Portbury KJ, Hardy MP, O'Leary DA, Kudoh J, Shibuya N, Shimizu N, Kola I, and Hertzog PJ (2004). Detailed mapping of the ERG-ETS2 interval of human chromosome 21 and comparison with the region of conserved synteny on mouse chromosome 16. *Gene* **324**, 65–77.
- [4] Zammarchi F, Boutsalis G, and Cartegni L (2014). 5' UTR control of native ERG and of Tmprss2:ERG variants activity in prostate cancer. *PLoS One* **8**e49721.
- [5] Wang J, Cai Y, Yu W, Ren C, Spencer DM, and Ittmann M (2008). Pleiotropic biological activities of alternatively spliced TMPRSS2/ERG fusion gene transcripts. *Cancer Res* **68**, 8516–8524.
- [6] Hagen R, Adamo P, Karamat S, Oxley J, Aninh JJ, Gillatt DD, Persdad R, Ladomery MR, and Rhodes A (2014). Quantitative analysis of ERG expression and its splice isoforms in formalin-fixed paraffin-embedded prostate cancer samples: association with seminal vesicle invasion and biochemical recurrence. *Am J Clin Pathol* **142**, 533–540.
- [7] Whyte MP (2010). Physiological role of alkaline phosphatase explored in hypophosphatasia. *Ann N Y Acad Sci* **1192**, 190–200.
- [8] Bonewald LF (2004). The amazing osteocyte. *J Bone Miner Res* **26**, 229–238.
- [9] Yarram S, Tasman C, Gidley J, Clare M, Sandy JR, and Mansell JP (2004). Epidermal growth factor and calcitriol synergistically induce osteoblast maturation. *Mol Cell Endocrinol* **220**, 9–20.
- [10] Gidley J, Openshaw S, Pring ET, Sale S, and Mansell JP (2006). Lysophosphatidic acid cooperates with 1 $\alpha$ ,25(OH)2D3 in stimulating human MG63 osteoblast maturation. *Prostaglandins Other Lipid Mediat* **80**, 46–61.
- [11] Blackburn J and Mansell JP (2012). The emerging role of lysophosphatidic acid (LPA) in skeletal biology. *Bone* **50**, 756–762.
- [12] Lancaster ST, Blackburn J, Blom A, Makishima M, Shizawa M, and Mansell JP (2014). 24,25-Dihydroxyvitamin D3 cooperates with a stable, fluoromethylene LPA receptor agonist to secure human (MG63) osteoblast maturation. *Steroids* **83**, 52–61.
- [13] Tigyis G and Mileli R (1992). Lysophosphatidates bound to serum albumin activate membrane currents in *Xenopus* oocytes and neurite retraction in PC12 pheochromocytoma cells. *J Biol Chem* **267**, 21360–21367.
- [14] Iwamoto M, Higuchi Y, Koyama E, Kurisu K, Yeh H, Abrams WR, Rosenbloom J, and Pacifici M (2000). Transcription factor Erg variants and functional diversification of chondrocytes during limb long bone development. *J Cell Biol* **150**, 27–40.
- [15] Yamamura K, Ohta Y, Mamoto K, Sugama R, Minoda Y, and Nakamura H (2018). Effect of eldcalcitol on articular cartilage through the regulation of transcription factor Erg in a murine model of knee osteoarthritis. *Biochem Biophys Res Commun* **495**, 179–184.
- [16] Mansell JP and Blackburn J (2013). Lysophosphatidic acid, human osteoblast formation, maturation and the role of 1 $\alpha$ ,25-dihydroxyvitamin D3 (calcitriol). *Biochim Biophys Acta* **1831**, 105–108.
- [17] Bustin SA, Benes V, Garson JA, Hellemans J, Huggett J, Kubista M, Mueller R, Nolan T, Pfaff MW, and Shipley GL, et al (2009). The MIQE guidelines: minimum information for publication of quantitative real-time PCR experiments. *Clin Chem* **55**, 611–622.
- [18] Sheridan DL, Kong Y, Parker SA, Dalby KN, and Turk BE (2008). Substrate discrimination among mitogen-activated protein kinases through distinct docking sequence motifs. *J Biol Chem* **283**, 19511–19520.
- [19] Jacobs D, Glossip S, Xing H, Muslin AJ, and Kornfeld K (1999). Multiple docking sites on substrate proteins form a modular system that mediates recognition by ERK MAP kinase. *Genes Dev* **13**, 163–175.
- [20] Selvaraj N, Kedage V, and Hollenhorst PC (2015). Comparison of MAPK specificity across the ETS transcription factor family identifies a high-affinity ERK interaction required for ERG function in prostate cells. *Cell Comm Signal* **13**, 12.
- [21] Fish JE, Cantu Gutierrez M, Dang LT, Khyza N, Chen Z, Veitch S, Cheng HS, Khor M, Antounians L, and Njock MS, et al (2017). Dynamic regulation of VEGF-inducible genes by an ERK/ERG/p300 transcriptional network. *Development* **144**, 2428–2444.
- [22] Iwamoto M, Higuchi Y, Enomoto-Iwamoto M, Kurisu K, Koyama E, Yeh H, Rosenbloom J, and Pacifici M (2001). The role of ERG (ets related gene) in cartilage development. *Osteoarthritis Cartilage* **9**, S41–S47.
- [23] Iwamoto M, Tamamura Y, Koyama E, Komori T, Takeshita N, Williams JA, Nakamura T, Enomoto-Iwamoto M, and Pacifici M (2007). Transcription factor ERG and joint and articular cartilage formation during mouse limb and spine skeletogenesis. *Dev Biol* **305**, 40–51.
- [24] Kiledjian M and Kadesch T (1990). Analysis of the human liver/bone/kidney alkaline phosphatase promoter in vivo and in vitro. *Nucl Acids Res* **18**, 957–961.
- [25] Weiss MJ, Ray K, Henthorn PS, Lamb B, Kadesch T, and Harris H (1988). Structure of the human liver/bone/kidney alkaline phosphatase. *Gene* **263**, 12002–12010.
- [26] Matsuura S, Kishi F, and Kajii T (1990). Characterization of a 5'-flanking region of the human liver/bone/kidney alkaline phosphatase gene: two kinds of mRNA from a single gene. *Biochem Biophys Res Commun* **168**, 993–1000.
- [27] Mansell JP, Cooke M, Read M, Rudd H, Shiel AI, and Wilkins K (2016). Chitinase 3-like 1 expression by human (MG63) osteoblasts in response to lysophosphatidic acid and 1,25-dihydroxyvitamin D3. *Biochimie* **128–129**, 193–200.
- [28] Meisel Sharon S, Pozniak Y, Geiger T, and Werner H (2016). TMPRSS2-ERG fusion regulates insulin-like growth factor-1 receptor (IGF1R) gene expression in prostate cancer: involvement of transcription factor Sp1. *Oncotarget* **7**, 51375–51392.
- [29] Kingsley LA, Fournier PG, Chirgwin JM, and Guise TA (2007). Molecular biology of bone metastasis. *Mol Cancer Ther* **6**, 2609–2617.
- [30] Chen F, Walder B, James AW, Soofer DE, Soo C, Ting K, and Zhang X (2012). NELL-1-dependent mineralisation of Saos-2 human osteosarcoma cells is mediated via c-Jun N-terminal kinase pathway activation. *Int Orthop* **36**, 2181–2187.